ISSN 0915-633X

NATIONAL INSTITUTE FOR FUSION SCIENCE

A New Boundary Control Scheme for Simultaneous Achievement of H-mode and Radiative Cooling (SHC Boundary)

N. Ohyabu

(Received - Mar. 31, 1995)

NIFS-356 May 1995

RESEARCH REPORT
NIFS Series

NAGOYA, JAPAN

A New Boundary Control Scheme For Simultaneous Achievement of H-mode and Radiative Cooling (SHC Boundary)

N.Ohyabu

National Institute for Fusion Science
Furho-cho, Chikusa-ku, Nagoya, 464-01, Japan

Abstract

We have proposed a new boundary control scheme (SHC boundary), which could allow simultaneous achievement of the H-mode type confinement improvement and radiative cooling with wide heat flux distribution. In our proposed configuration, a low m island layer sharply separates a plasma confining region from an open "ergodic" boundary. The degree of openness in the ergodic boundary must be high enough to make the plasma pressure constant along the field line, which in turn separates low density plasma just outside the plasma confining region (the key external condition for achieving a good H-mode discharge) from very high density, cold radiative plasma near the wall (required for effective edge radiative cooling). Examples of such proposed SHC boundaries for Heliotron typed devices and tokamaks are presented.

1. Introduction

The major issue in the ITER design study is how to handle high heat flux (~ 400MW α power) reliably, while maintaining a high quality core plasma, i.e., a good H-mode and nearly pure plasma [1]. Despite intensive efforts, no convincing scenario has emerged so far. For reduction of the heat flux on the divertor plate (the present ITER design goal: 5 MWm^{-2} [1]), the heat flux must be converted into the impurity radiative power to distribute the heat flux over a surface area as large as ~ 1/5 of the total plasma surface. But this is generally contradictory to achievement of a high quality plasma, especially an H-mode plasma [2] (a confined plasma with enhanced energy confinement).

In the late 70s , the expanded boundary concept [3] was proposed, in which a large volume of the radiative cooling region allows effective edge cooling. The key ingredients of the concept are : *(i) a large cooling volume of the special edge magnetic configuration, (ii) constant pressure in the "open" boundary, (iii) impurity retention within the boundary by the plasma flow.* They all enhance edge impurity radiative cooling. But no consideration on the H-mode was made since the energy confinement was believed to be good. Two edge magnetic configurations were proposed as expanded boundaries, a poloidal divertor with a large expansion of the divertor channel (Fig.1(a)) [3] and an ergodic boundary with a large radiative boundary volume (the ergodic boundary or limiter was originally proposed to enhance the particle convection just in front of the wall and hence lower the edge temperature there [4]). The former configuration, called the expanded boundary poloidal divertor, were tested in the DoubletIII device [5,6]. Expansion of the divertor channel, however, was modest, as depicted in Fig.1(b) [6], compared with the originally proposed one (Fig.1(a)). Yet the experiment demonstrated (i) the existence of the cold, high density divertor plasma near the divertor plate due to the constant pressure effect [5], (ii) very effective argon retention within the divertor channel under certain conditions [6]. Soon after the discovery of the H-mode in ASDEX with a closed poloidal divertor [2], "H-mode" was also achieved in Doublet III with the expanded boundary divertor [7]. Unlike ASDEX H-mode discharges, τ_E is a factor of two higher than that of the comparable limiter discharge even without the L-H transition. But the absolute value of τ_E is not as high as that of ASDEX H-mode discharge with the same plasma current. It is believed to be due to difference in recycling control capability between "open" and "closed" divertors. With higher beam power, however, the transition did appear with slight additional enhancement

of τ_E. It was found that the divertor plasma plugging (i.e., divertor plasma prevents the neutrals recycled at the divertor plate from penetrating into the edge of the main plasma by ionizing them.) is the key in achieving an H-mode in open divertors such as the expanded boundary poloidal divertor. In DIII-D (the upgrade device of Doublet III), H-mode discharges with a clear transition were achieved [8] with divertor configuration, which is no longer expanded boundary divertor. Larger size of DIII-D, however, makes the plasma plugging very effective even with small size of the divertor channel relative to the main plasma size. It has also demonstrated simultaneous achievement of H-mode and radiative cooling [9], the key divertor operational scenario of ITER. Separation of the low density SOL plasma just outside the last closed flux surface (LCFS) from the high density cold radiative plasma in the divertor channel appears to be essential for this, otherwise incompatible. Yet its straightforward extrapolation to ITER is very unlikely because of significantly higher heat flux in ITER. The expanded boundary approach, which was proposed as an edge radiative cooling scheme for reactor grade devices, revisit with an H-mode consideration. The configuration with large expansion of the divertor channel, shown in Fig.1(a) will be more effective in diverting the heat flux over a large surface area. Expansion of the divertor channel, however, requires many poloidal coils located inside the toroidal coil cage, which may not be attractive from the reactor engineering point of view. An ergodic boundary, an alternative expanded boundary will be more acceptable to the reactor engineering because of much lower required coil currents and thus simpler coils. In this paper, we propose a new kind of "ergodic" boundary (SHC boundary), which could allow simultaneous achievement of a good H-mode and radiative cooling with wide heat flux distribution.

2. Conditions for constant pressure in the open region.

Constant pressure along the field line derived from the parallel plasma momentum balance is the key mechanism to separate two regions, low density plasma region and high density cold plasma region even though they are connected each other through the field lines. We examine whether the constant pressure holds in the open surface region since it is one of the critical physics mechanisms in the proposed SHC boundary.

First we attempt to find a condition for the constant pressure in the

poloidal divertor channel even though it has been validated by the experimental observations. When the temperature is below ~ 5 eV near the divertor plate, the hydrogen atomic processes play important roles in the energy and momentum balances, lowering the plasma pressure near the plates. It has been argued that reduction of the pressure is the key condition for decrease in the heat flux to the divertor plate to an acceptable level, otherwise too much recombination power to the plates [1]. In a divertor channel region which is several ionization mean free path away from the divertor plate, however, the constant pressure must hold to maintain high density for enhancement of the radiative loss and hence cooling of the divertor plasma down to 5 ~ 10 eV. Here we consider an effect of E×B drift on the constant pressure in such a divertor region. A simple dimensional analysis is given here, using a very simplified divertor geometry, as shown in Fig.2(a) where x is the radial coordinate with the separatrix located at x = 0 and y is the coordinate along the poloidal direction. In the SOL, the electric potential (φ) along the field line is determined by the electron parallel momentum equation (i.e.,the electric field term is balanced by the the thermal force term) and is approximately given by $\varphi(y) \approx \alpha T(y)$ (where α is 0.71) and the potential at different radii (x) are then determined by the fact that the field lines are connected to the divertor plates with electrically grounded (i.e.,$\varphi = 0$). We also assume that the potential difference near the plate is small since the electron temperature there is low. The particle fluxes along the x and y directions (Γ_x,Γ_y) are given by $\Gamma_x = - nE_y / B$, $\Gamma_y = \theta nu_{\parallel} + nE_x / B$, respectively (where $\theta = B_p$ (poloidal field) / B). Since div $\Gamma \approx 0$ in the region of our interest, the parallel plasma flow ($u_{\parallel}$) is the order of $\sim - \alpha T / e\Delta_T \theta B \approx -\alpha(\rho_i / \theta\Delta_T)v_{thi}$ where ρ_i is the ion Larmor radius, v_{thi} is the ion thermal velocity and Δ_T^{-1} is $|(\partial T/\partial x)/T|$. Then the viscous force associated with the induced parallel flow changes the parallel momentum balance, described as follow .

$$- 2\nabla_{\parallel}(nT) + \nabla_{\perp}(D^*\nabla_{\perp}(Mnu_{\parallel})) = 0 \qquad (1)$$

where D* is the viscosity . Assuming that $\nabla_{\perp}(D^*\nabla_{\perp}(Mnu_{\parallel})) \approx MD^*nu_{\parallel} / \Delta_v^2$, the constant pressure assumption is valid if

$$L\nabla_{\parallel}(nT) / nT \approx \alpha(\rho_i / \theta\Delta_T) \{(LD^* / v_{thi})^{1/2} / \Delta_v\}^2 << 1 \qquad (2)$$

For the present typical poloidal divertor experiment ($\rho_i \approx 1$ mm, $\theta \approx 0.1$, $\Delta_T \approx 10$ mm, thus $(\rho_i / \theta\Delta_T) \approx 1$), the constant pressure assumption has been validated by the observations, indicating that $(LD^* / v_{thi})^{1/2} / \Delta_v \leq 1$. For different configurations with much lower equivalent θ, such as the island divertor (illustrated in Fig.2(b)), θ is as small as $\sim 8\times10^{-3}$ instead of 0.1 and thus the condition may not be satisfied. If Δ_T scales as $\theta^{-1/2}$, $\theta\Delta_T$ may scale as $\theta\Delta_T \propto \theta^{1/2}$. For the case of $\theta = 8\times10^{-3}$, the constant pressure condition is satisfied when $(LD^* / v_{thi})^{1/2} / \Delta_v \leq 0.5$. This argument is very crude, requiring a detailed theoretical study or experimental study for more definitive discussion.

Next we examine the constant pressure assumption in the ergodic boundary, which has not been demonstrated experimentally. The first ergodic boundary experiment was done in TEXT Ohmic discharges [10]. It demonstrated that the edge temperature can be reduced without affecting the core plasma. Recent ergodic boundary experiment in the larger device, Tore Supra [11] shows that the edge radiative cooling can be achievable at relatively low average core density even with auxiliary heating power. However, these experiments have not generated an inversion of the density profile in the ergodic boundary, which the observed normal temperature gradient there expected to accompany through the effect of the constant pressure in the ergodic boundary. This may be due to high anomalous diffusion and viscosity [12] or ion-neutral collision, as discussed below.

In the ergodic boundary, the temperature profile is determined mainly by the electron parallel thermal conductivity and the power dissipation. For simplicity, we assume the temperature profile as illustrated in Fig.3(a). The radial particle flux ($\Gamma_r(r)$) in a steady state is determined by div Γ = S (particle source) and is high near the wall and becomes low beyond the ionization zone. The Γ_r consists of the anomalous diffusion ($- D \nabla_\perp n$) and the parallel flow ($nu_\parallel$),

$$\Gamma_r(r) = - D \nabla_\perp n + \langle \delta b / B \rangle n u_\parallel \qquad (3)$$

where $<\delta b / B>$ is the average angle of the field line toward the radial direction. This parallel flow may cause parallel momentum loss due to the anomalous viscosity and the ion -neutral collision, described as

$$-\nabla_{\parallel}P - Mn D^{*} \nabla_{\perp}^{2} u_{\parallel} - Mn\nu u_{\parallel} = 0 \qquad (4)$$

where M is the mass of the bulk ion and D^{*} and ν are the viscosity and the ion-neutral collision frequency, respectively. Replacing $\nabla_{\perp}^{2}$ and $\nabla_{\parallel}$ by Δ^{-2} and $<\delta b / B>\nabla_{\perp}$ respectively, Eq.(4) becomes

$$n u_{\parallel} = -<\delta b / B>\nabla_{\perp}P \; / \; M(D^{*}\Delta^{-2}+\nu) \qquad (5)$$

Eliminating $nu_{\parallel}$ from Eqs.(3) and (5), we obtain

$$-\nabla_{\perp}P / P = (\Gamma_{r}+D\nabla n)M(D^{*}\Delta^{-2}+\nu) \; / \; 2nT<\delta b / B>^{2} \qquad (6)$$

Here $P = 2nT$ is assumed. Eq.(6) is rewritten as

$$\nabla_{\perp}n / n = [-\nabla_{\perp}T /T - \eta \Gamma_{r} / nD] \; / \; (1+\eta) \qquad (7)$$

where $\eta = D(D^{*}\Delta^{-2}+\nu) \; / \; v_{thi}^{2}<\delta b / B>^{2}$. The density scale length $(\nabla_{\perp}n / n)^{-1}$ is plotted as a function of η in the Fig.3(b). When $\eta << 1$, $\nabla_{\perp}n / n \approx -\nabla_{\perp}T /T$, i.e., the constant pressure assumption is valid. For the opposite extreme case ($\eta >> 1$), the conventional relation $\Gamma_{r} \approx -D\nabla_{\perp}n$ is recovered.

For the TEXT parameters [10] ($<\delta b / B> = 1\times10^{-3}$, $\Delta \sim 2$ cm, $v_{thi} \sim 3\times10^{4}$ m/s), the constant pressure assumption ($\eta < 0.5$) is valid only when $(DD^{*})^{1/2}$ is less than 0.4 m^{2}/s. Furthermore, even with low D, e.g. D = 0.1 m^{2}/s, the neutral density must be below 3×10^{11} cm^{-3}. The edge transport coefficient $(DD^{*})^{1/2}$ in the small tokamaks is probably higher than this value and thus it appears to be more reasonable not to observe an inversion of the density profile in TEXT. For larger devices with higher magnetic field (larger Δ , and higher v_{thi}, smaller $(DD^{*})^{1/2}$), the requirement on $<\delta b / B>$ is relaxed substantially.

3. Concept of SHC Boundary

In our proposed configuration, the plasma confining region with perfect magnetic flux surfaces is sharply separated by an open ergodic region. Examples of such configurations for Heliotron type helical devices and circular tokamaks are presented in Sec.4 and 5, respectively. The degree of openness must be high enough to make the plasma pressure constant along the field line in the open region. And thus a drop of the temperature accompanies an increase in density toward the wall, thereby allowing separation between low density plasma just outside the LCFS and high density divertor plasma near the divertor plate or wall. High density plasma in the boundary with a large volume enhances the radiative cooling power with wider heat flux distribution and localizes the particle recycling within the outer boundary.

Whether the proposed concept work depends on the true H-mode condition. Experimentally, low recycling is favorable for H-mode formation itself and the H-mode quality. High recycling, if localized in the divertor region is still acceptable, as shown in DIIID experiment [9]. These facts suggests that low density at the SOL surrounding the main plasma region or possibly small density scale length ($L_n = (1/n)(dn/dr)$) just inside the LCFS is the key H-mode condition, which can be imposed externally. Appearance of the H-mode thermal barrier only at the very edge of the closed surface is also consistent with the above argument since L_n can be small only there.

The importance of small L_n is also supported by a popular model for the H mode, based on the shear of the radial electric field [13]. In the DIII helium H-mode discharges, the E_r (negative during H-phase) is mainly from the ∇P term in the radial momentum balance of ions and the bulk ions rotate in the ion diamagnetic direction, contributing to reduce $|E_r|$ [14]. Thus dE_r/dr is given as $\sim -(1 / eBn^2)(dn/dr)(dP/dr)$ where d^2P/dr^2 are assumed to be small. Small L_n makes dE_r/dr high and hence possibly suppresses the plasma turbulence responsible for the L-mode edge transport.

In the conventional ergodic boundary, imposed by high m external resonant fields [10,11], Eq.(7) predicts constant pressure in the outer region of the boundary where $<\delta b / B>$ is high enough. But in the inner ergodic

boundary region near the LCFS, Smaller $<\delta b / B>$ still causes high electron thermal diffusivity, thus preventing appearance of the H-mode thermal barrier, but the pressure may not be constant, resulting in the normal density gradient and hence higher density at LCFS. This is unfavorable for generation of a good H-mode. When a single low m island layer is imposed in this region by the external resonant helical coils, it shortcircuits the inner ergodic boundary and thus connect the LCFS to the outer ergodic boundary with constant pressure, as illustrated in Fig.4. It is important to note that with low m resonant field, the satellite islands with poloidal mode number of $m \pm 1$ appearing in the closed region due to the toroidal coupling, can be cancelled easily by the additional correction coils (this is not true for the high m case).

4. SHC boundary for the Large Helical Device (LHD)

The National Institute for Fusion Science (NIFS) is constructing a large, heliotron type device (l=2, m=10, R = 3.9 m, <a> = 0.6 m, B = 4 T) [15,16], called the Large Helical Device (LHD), aimed at demonstrating the attractiveness of the helical device at more reactor relevant plasma parameters. Its detailed design specifications are given elsewhere [16]. It is equipped with a natural helical divertor configuration [17], which is the key element of the device, particularly for achieving high quality helical plasmas. Unlike tokamak poloidal divertor configuration, the open edge region has a complicated three dimensional structure, as described below and its thickness with strong poloidal variation increases as the plasma moves outwards or the plasma β value increases. It has n=10 toroidal symmetry and generates natural island layers with toroidal mode number of 10 in the edge region. The radial locations and widths of the natural islands on the inner midplane at $\phi = 0^{\circ}$ for the standard case with R_{axis}(the position of the plasma axis)= 3.75 m (the center of the two helical coils is located at R = 3.90 m) and the case with R_{axis} = 3.85 m are shown in Fig.4(a),(b), where the connection lengths (the field line lengths between the starting point and the divertor plate) are plotted as a function of the starting location on the inner midplane. With increasing radius, island layers with poloidal mode number of 11, 10, 9, 8, 7, appear successively with increasing island width. The island layers with lower m overlap, generating stochastic field region. Beyond this stochastic region, there is an "edge surface layer" [17] peculiar to the Heliotron type helical divertor configuration. For outward shifted or high β discharges, the

natural boundary layer is quite thick and the definition of the LCFS becomes very vague. When the resonant field is imposed to generate a m/n=1/1 island, the complicated boundary becomes much simpler. The isolated island layers and a part of a stochastic region are buried within the imposed n/m=1/1 island, as shown in Fig.4(c) (Fig.4(d)) where the O-point (X-point) of the n/m=1/1 island is on the inner midplane (at R ~ 3.38 m and Z=0). Fig.4(e) shows a Poincare plot of the field line on the poloidal plane where the X-point of the island is located on the inner midplane. With the n/m=1/1 island, the LCFS can also be clearly defined within ~ 2 mm and the connection length just outside of the LCFS is ~ 200 m (~ $8\times 2\pi$ R), an ideal SHC boundary configuration. In addition, an n/m =1/1 island may be beneficial for the τ_E enhancement for some unknown reasons since " H-mode" so far has been achieved only when ι at the LCFS is very close to 1.0 or 0.5 (the major rational surfaces) in stellarator devices, W7AS [18] and CHS [19] (two quite different devices in terms of magnetic confining geometry). Thus the LHD configuration with n/m=1/1 island will probably achieve an H-mode and radiative cooling simultaneously.

5. SHC boundary for tokamaks

For tokamaks, which have ι-profiles quite different from that of LHD, an island layer with n/m=1/4 may be a good choice for a separator between the closed surface and the open regions. We use three sets of coil to generate a tokamak SHC boundary. The main coil set (referred to as the m=5 coil set) generates an n/m=1/5 primary island layer as well as a satellite n/m=1/4 island layer. Thus overlapping of m=4 and m=5 island layers creates an ergodic boundary. Island layers with n/m=1/3 and1/2 are also generated by the m=5 coil set, even though they are small. Other two sets of coils (m=3 and m=2 correction coil set) are fine tuning coil sets which reduce the size of m=3 and m=2 islands to an acceptable level, respectively.

To substantiate the above arguments, we analytically demonstrate that a SHC configuration can be created in a circular tokamak by the above mentioned three coil sets. First we assume that the toroidal effects are weak in our approximation, i.e., $\varepsilon = a / R << 1$ and retain the terms with order ε. When a resonant helical field with mode number m and n is imposed to a circular tokamak equilibrium, the radial motion of the the field line is described by

$$dr/d\phi = (R_o / B_{\phi o})\, b(r) \cos [m\alpha - n\phi] [1 + (2 r / R_o) \cos\alpha] \qquad (8)$$

where $b(r) \cos [m\alpha - n\phi]$ is the radial component of the resonant field, R_o is the major radius of the center of the flux surface, which resonates with helical fields and $B_{\phi o}$ is the toroidal field at the flux surface center. Here we use a toroidal coordinate (r(radius),α(the poloidal angle),ϕ(the toroidal angle)) with the major radius of the axis $R = R_o$. However, in this coordinate, the field lines are not described as a linear function of α and ϕ. Then a new poloidal angle ($\theta = \alpha - (r/R_o) D \sin\alpha$) is introduced in such a way that the field lines are described by the linear relation $\theta = \phi / q$. Here D is approximately equal to $1 + \beta_p + l_i / 2$ for the edge region and q, β_p, l_i are the q-value, the poloidal beta and the internal inductance, respectively. Even with a perturbation field, the relation $\theta = \phi / q$ of the field line is still valid in our approximation because the perturbed poloidal field of our interest is ~ 1 % of the equilibrium poloidal field. The radial motion of the the field line is described by

$$\begin{aligned} dr/d\phi = {} & b(r) R_o / B_{\phi o} \{ \cos(m\theta - n\phi) \\ & + (r/R_o) [(m/2) (1 + \beta_p + l_i /2) + 1] \cos[(m+1)\theta - n\phi] \\ & + (r/R_o) [- (m/2) (1 + \beta_p + l_i /2) + 1] \cos[(m -1)\theta - n\phi] \} \end{aligned} \qquad (9)$$

Here we use the following approximation : $\cos(\Theta + z \sin\theta) \approx \cos\Theta + (z/2) \cos (\Theta+\theta) - (z/2) \cos(\Theta-\theta)$ when $z \ll 1$. From Eq.(4) and the relation $\theta = \phi / q$, the half width of m/n island ($\delta_{1/2}(m)$), generated by resonant helical field, is estimated as

$$\delta_{1/2}(m) = [(4R_o b(r) / nB_{\phi o})(q/q')]^{1/2} \qquad (10)$$

and the sizes of satellite islands with m+1,m-1 are estimated similarly.

We consider continuous helical coils wound on the circular toroidal tube surface(the major radius : $R_o - d$, the minor radius: a_c) with the pitch modulation (ξ). Here d represents the shift between the center of the flux surface and that of the coil tube. They generate the radial component of magnetic field, approximately given as

$$b_\rho \approx b_o (\rho / a_c)^{(m-1)} \cos [m (\omega + \xi \sin\omega) - n \phi] \qquad (11)$$

where a toroidal coordinate (ρ, ω, ϕ) with the major radius of $R = R_o - d$ is used. The relations between two toroidal coordinates (ρ, ω, ϕ) , (r, α, ϕ) are given as

$$\rho e^{i\omega} = r e^{i\alpha} + d = r e^{i\alpha} (1 + (d/r) e^{-i\alpha}) \qquad (12)$$

The radial field now can be rewritten using the (r, α, ϕ) coordinate,

$$b_r \approx b_o (r / a_c)^{(m-1)} \mathrm{Re} \{ e^{i(m\alpha - n\phi)} + m\xi/2 \; e^{i[(m+1)\alpha - n\phi]} + (md/r - m\xi/2) e^{i[(m-1)\alpha - n\phi]} \} \qquad (13)$$

Here we retain md/r term as order of ε, but drop d/r terms.

The sizes of the island, generated by a set of helical coil current (the mode numbers m/n , the pitch modulation ξ and the shift (d) between the centers of the flux surface and coil winding tube surface are given from Eq(4) and (8),

$$\delta_{1/2}(m+1) / \delta_{1/2}(m) \approx (r_{m+1} / r_m)^{(m-1)/2} \times | m\xi/2 + (r/R_o) [(m/2) (1 + \beta p + li /2) + 1] |^{1/2}$$

$$\delta_{1/2}(m-1) / \delta_{1/2}(m) \approx (r_{m-1} / r_m)^{(m-1)/2} \times | md/r - m\xi/2 + (r/R_o) [-(m/2) (1 + \beta p + li /2) +1] |^{1/2} \qquad (14)$$

where r_m and $r_{m\pm1}$ are the radii of the q = m/n and $(m \pm 1)/n$ rational surfaces, respectively.

From these formula, an optimum pitch modulation (ξ) and shift (δ) are determined. With the m=5 coil set, the m=4 island is used to separate sharply the closed region from the open surface region and the m=5 and 6 island layers are overlapped, generating an ergodic boundary. If one want even larger volume of the boundary, the m=7 island layer can be available. This coil set does not generate a m=3 island layer in our approximation, but it actually generates a small m=3 island and there must exist an optimum ξ for

minimizing m=3 island size. For fine tuning coil (m=3,m=2) sets for minimizing the size of unwanted m=3,2 islands, ξ and δ should be chosen to minimize the size of the $(m \pm 1)$ satellite island from Eq (9). Thus we can conclude that the above coil sets generate an ergodic (SHC) boundary in circular tokamaks, suitable for simultaneous achievement of the H-mode and radiative cooling.

6. Discussions

We have proposed a new ergodic boundary concept which could allow simultaneous achievement of H-mode and radiative cooling. In the proposed configuration, the plasma confining region is sharply separated from the open boundary region with constant pressure. This allows relatively low density at the last closed flux surface, while maintaining cold, high density plasma in the outer open boundary region. Large volume of the boundary reduces the required impurity relative concentration (n_{im}/n_e) for the radiative cooling down to an acceptable level, e.g. the order of that in the core [20]. Furthermore it helps to distribute the heat flux over a large wall surface, reducing the heat load significantly. As discussed in Sec.3, achievement of a high quality H-mode discharge requires low density at the SOL surrounding the core plasma, which is generally contradictory to the edge radiative cooling. For ITER grade devices with average density (1×10^{14} cm^{-3}), the density at the SOL (n_{sol}) may be required to be ~ 3×10^{13} cm^{-3} for achieving a good H-mode discharge and the electron temperature in the SOL(T_{sol}) is expected to be 200 ~ 300 eV for the expected fusion α power. Separation between the low density plasma in the SOL and high density plasma in the divertor channel near the divertor plate requires a drop of the temperature along the field line under the constant pressure condition. The temperature drop can exist if

$$\lambda_e/L < 0.8\ (m/M)^{1/2}\ \gamma \qquad (15)$$

where m and M are the electron and ion masses, respectively, γ is the heat transmission coefficient at the sheath and λ_e is the electron mean free path (this requirement is given in Ref.[5], but in a different parametric form). For a case close to the ITER parameters ($n_{sol} = 3\times10^{13}$ cm^{-3}, T_{sol} = 300 eV), λ_e is 30 m , thus requiring that L > 300 m. For an reactor grade LHD ($<\delta b / B> = 1\times10^{-3}$, Δ ~ 0.2 m, T ~ 100 eV), the connection length (L) is ~ 800 m, satisfying the condition (15) easily. The constant pressure condition ($\eta < 0.5$

) is given in Sec.2 where $\eta = D(D^*\Delta^{-2}+\nu) / v_{thi}^2 < \delta b / B >^2$. The viscous term is small and the collision term determines the parallel pressure gradient, requiring that the neutral density (n_0) is below 1×10^{11} cm^{-3} for $\eta < 0.5$. This condition is also easily satisfied in the boundary region inside of the ionization zone.

For the tokamak configuration, described in Sec.5, we consider the case where the m=4 and m=5 islands barely overlap rather than complete overlapping. In this case, the minimum connection length is approximately the distance which the field line circulate one of the island, approximately 4 m times toroidal circumference. Thus the condition(15) is easily satisfied. A tokamak SHC boundary, described in Sec.5 are somewhat closer to poloidal divertors or island divertors, illustrated in Fig.2(b) rather than the SHC boundary, described in Sec.3 (a fine ergodic boundary combined with a low m island layer) i.e., the field line moves more or less orderly with effective θ of $\sim 8 \times 10^{-3}$. In these configurations, the temperature will certainly drop along the field line in the open boundary. The condition of the constant pressure, however, may not be guaranteed, as described by Eq.(2), motivating an experimental study. In the present large tokamak divertor with the divertor connection length of ~ 100 m for high q operation ($\theta \sim 8 \times 10^{-2}$), there is no counter evidence against validity of the constant pressure assumption. Accordingly, even for an ITER class SOL plasma of $n_{sol} = 3 \times 10^{13}$ cm^{-3} and $T_{sol} = 300$ eV, very high density near the wall probably be maintained even in these configurations with effective θ of $\sim 8 \times 10^{-3}$.

Recently the ITER team has proposed Dynamic Gas Divertor Operation [1], in which the majority of radiation and ionzation take place in the middle of the divertor channel, reducing the heat load to the divertor target plates. Such a state is called "detached plasma". For the present large devices such as JET and JT60U, divertor plasma is detached from the target plates, but highly radiative area is located near the X-point within the separatrix. Thus this appears to prevent formation of the H-mode discharge since it cool down the temperature just within the separatrix. If the m/n=4/1, 5/1 island layers exist just inside the separatrix of the poloidal divertor configuration, the LCFS moves inwards, i.e., the separatrix of the m=4 island becomes the LCFS and plasma with modest density and relatively high temperature at the new LCFS may be separated from high density, cold radiative plasma in the very edge,

achieving H-mode and detached plasma simultaneously.

In summary, we have proposed a new boundary control scheme (SHC boundary), which could allow simultaneous achievement of the H-mode type confinement improvement and edge radiative cooling with wide heat flux distribution. In our proposed configuration, the plasma confining region is sharply separated from an open ergodic boundary with constant pressure.

ACKNOWLEDGEMENTS

I would like to express my particular appreciation to Academician B Kadomtsev for his valuable comments and Profs. A.Iiyoshi, M.Fujiwara and O.Motojima for continuous encouragement throughout this study. I like to thank Dr.T.Morisaki who has done numerical calculations of the LHD SHC boundary.

REFERENCES

[1] JANESCHITZ,G., BORRASS, K., FEDERICI,G., et al.,Proc. of 11 th Inter. Conf. Plasma wall Interactions, Mito (1994) (to appear in J. Nucl. Mater.).

[2] WAGNER,F., BECKER,G., BEHRINGER,K., et al., Phys. Rev. Lett. 49 (1982) 1408.

[3] OHYABU,N., Nucl. Fusion 21 (1981) 519.

[4] FENEBERG,W., WOLF,G.H., 21, Nucl. Fusion (1981) 669.

[5] MAHDAVI,M.ALI, DEBOO,J.C., HSIEH,C.L., OHYABU,N., STAMBAUGH,R.D., WESLEY,J.C., Phys. Rev. Lett. 47 (1981) 1602.

[6] OHYABU,N., DEBOO,J.C., GROEBNER,R.J., MAHDAVI,M.ALI, TAYLOR,T., WESLEY,J.C., Nucl. Fusion 23 (1983) 295.

[7] OHYABU,N., BURRELL,K.H., DEBOO,J., et al., Nucl. Fusion 25 (1985) 49.

[8] BURRELL,K.H., EJIMA,S., SCHISSEL,D.P., et al., Phys. Rev. Lett. 59 (1987) 1432.

[9] PETRIE,T.W., APS-DDP meeting, 1993, St. Louis, Mo (to appear in Physics of Fluid, 1994).

[10] OHYABU,N., deGRASSIE,J.S., BROOKS,N., TAYLOR,T., IKEJI,H., et al., Nucl. Fusion 25 (1985) 1984.

[11] GROSSMAN,A., GHENDRICH,P., DEMICHELIS,C., MONIER-GARBET,P., VALLET,J.,C., et al., J. Nucl. Mater. 196-198 (1992) 59.

[12] SAMAIN,A, GROSMAN,A., BLENSKI,T., et al., J. Nucl. Mater. 128-129 (1984) 395.

[13] BIGLARI,H., DIAMOND, P.H.,KIM,K.M., et al. in Plasma Physics and Controlled Nuclear Fusion Research 1990 (Proc.13th Int. Conf. Washington, 1990), Vol. 2, IAEA, Vienna (1991) 191.

[14] KIM, J., BURRELL, K.H.,GOHIL, P., et al., Plasma Physics and Controlled Fusion 36 (1994) 183.

[15] IIYOSHI,A., FUJIWARA, M., MOTOJIMA, O., OHYABU, N. and YAMAZAKI, Fusion Technology 17 (1990) 169.

[16] MOTOJIMA,O.,AKAISHI,K.,FUJII,K.,FUJIWAKA,S.,IMAGAWA,S., et al., Fusion Engineering and Design 20 (1993) 3.

[17] OHYABU,N., WATANABE,T., JI,H., AKAO,H., ONO,T., et al., Nucl. Fusion 34 (1994) 387.

[18] ERCKMANN,V., WAGNER,F., BALDZUHN,J., et al.,., Phys. Rev. Lett. 70 (1993) 2086.

[19] TOI, K., OKAMURA, S., IGUCHI, S., et al., in Plasma physics and Controlled Nuclear Fusion Research 1992 (Proc.14th Int. Conf. Wurzburg, 1992), Vol. 2, IAEA, Vienna (1993) 461.

[20] OHYABU,N., DEGRASSIE,J.S., Nucl. Fusion 27 (1987) 2171.

Figure Captions

Fig.1

(a)Expanded boundary configuration proposed in [3]

(b)Expanded boundary poloidal divertor in Doublet III

Fig.2

A simplified poloidal (a) and island (b) divertor geometries.

Fig.3

(a) Schematic profiles of the temperature (T(r)), the normalized resonant field amplitude($<\delta b / B>$) and the radial particle flux ($\Gamma(r)$) in the ergodic boundary

(b) The density scale length as a function of

$\eta = D(D^*\Delta^{-2}+\nu) / v_{thi}^2 <\delta b / B>^2$ where D : diffusivity,

D^* : viscosity, Δ : the radial width of the ergodic structure,

ν : the ion-neutral collision frequency, $L_T = |\nabla T/T|$

Fig.4

Expected density and temperature profiles in the SHC boundary

(a) Schematic geometry of the proposed SHC Boundary.

(b)The electron thermal diffusivity (χ_{erg}) induced by the ergodic structure is plotted as a function of radius. The value of χ_{erg} is high at the island because it flattens the profiles.

(c) Expected density and temperature profiles in the ergodic (SHC) boundary.

Fig.5

An SHC boundary geometry of LHD

(a) the connection length is plot as a function of the position on the inner midplane for the standard LHD configuration (R_{axis}=3.75 m)

(b) R_{axis}=3.85 m

(c) An SHC boundary geometry of LHD with n/m=1/1 island at the edge. The island O-point is close to the starting point on the inner midplane. R_{axis}=3.85 m

(d) The same configuration as (c). The island X-point is close to the starting point on the inner midplane

(e) the field line Poincare plot on the poloidal plane with the same starting points as (d).

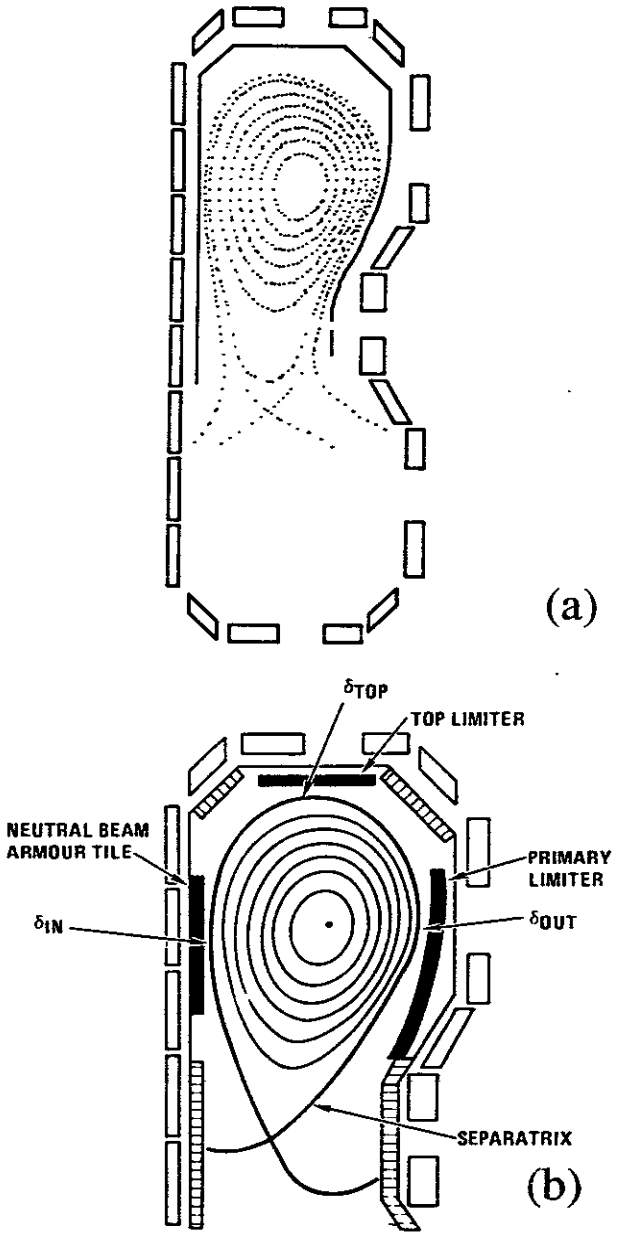
(a)
δ_{TOP}
TOP LIMITER
NEUTRAL BEAM
ARMOUR TILE
PRIMARY
LIMITER
δ_{IN}
δ_{OUT}
SEPARATRIX
(b)

Fig.1

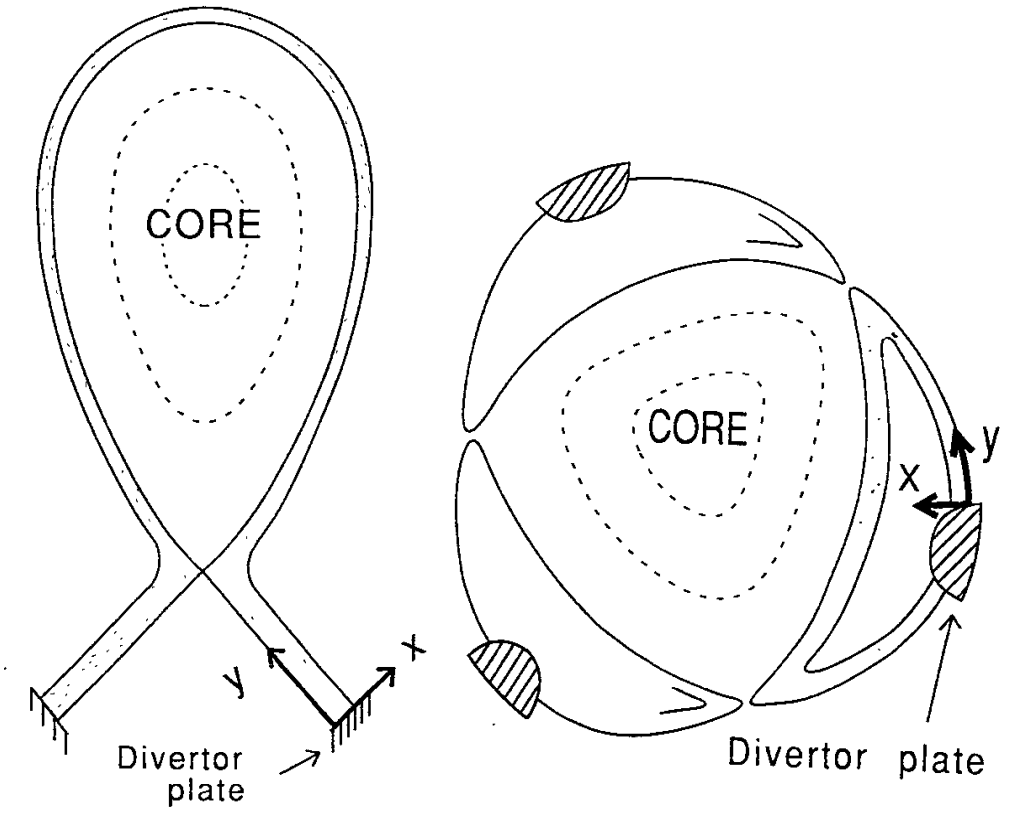

(a) (b)

Fig.2

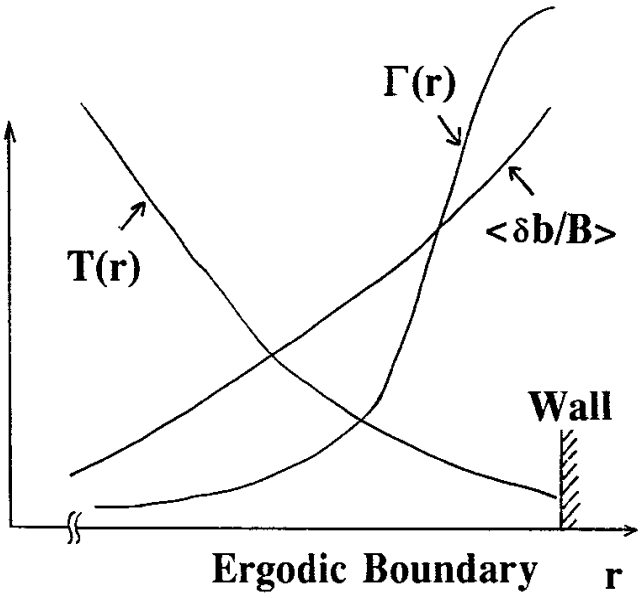

(a)

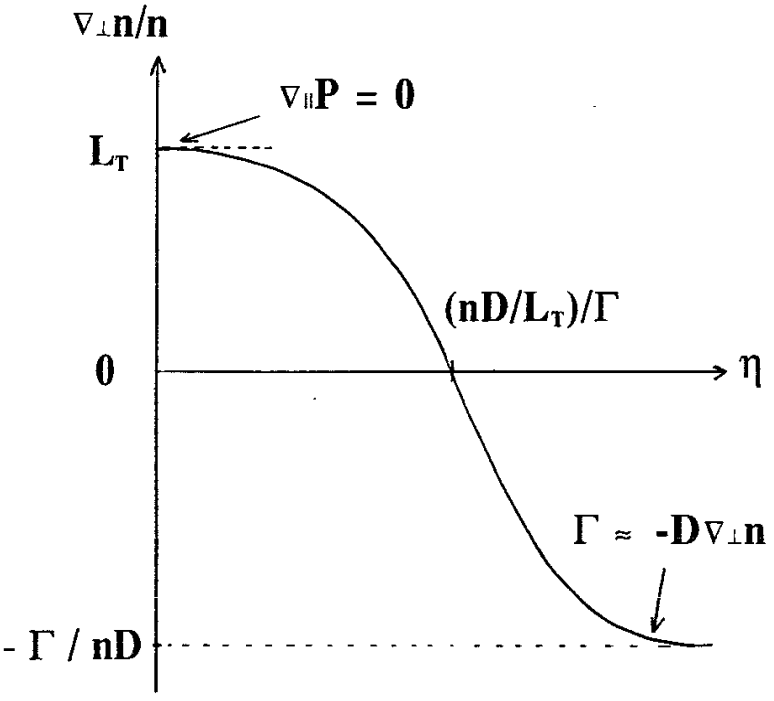

(b)

Fig.3

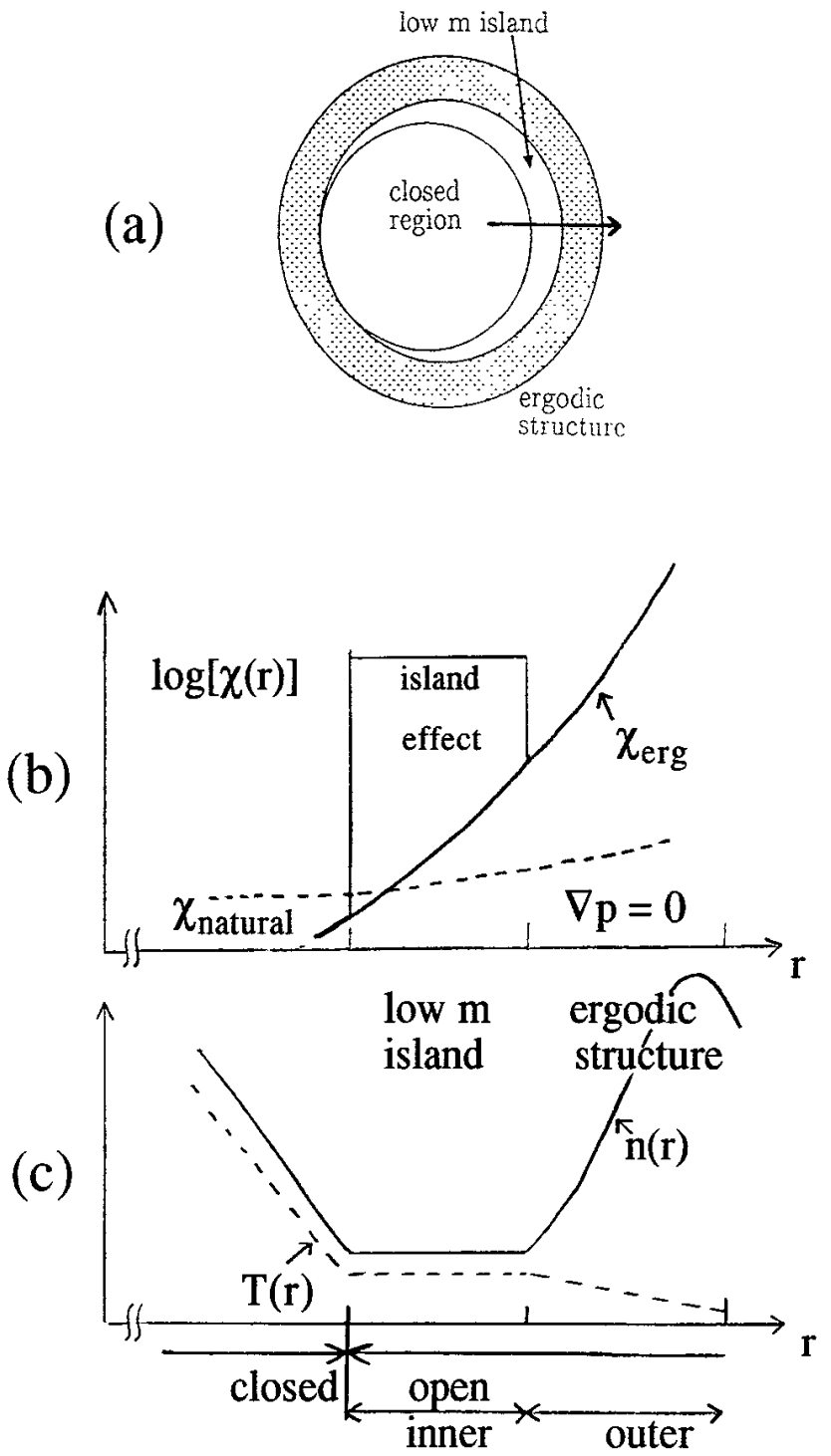
(a)
low m island
closed region
ergodic structure
(b)
log[χ(r)]
island effect
χerg
χnatural
∇p = 0
r
(c)
low m island
ergodic structure
n(r)
T(r)
r
closed
open
inner
outer

Fig.4

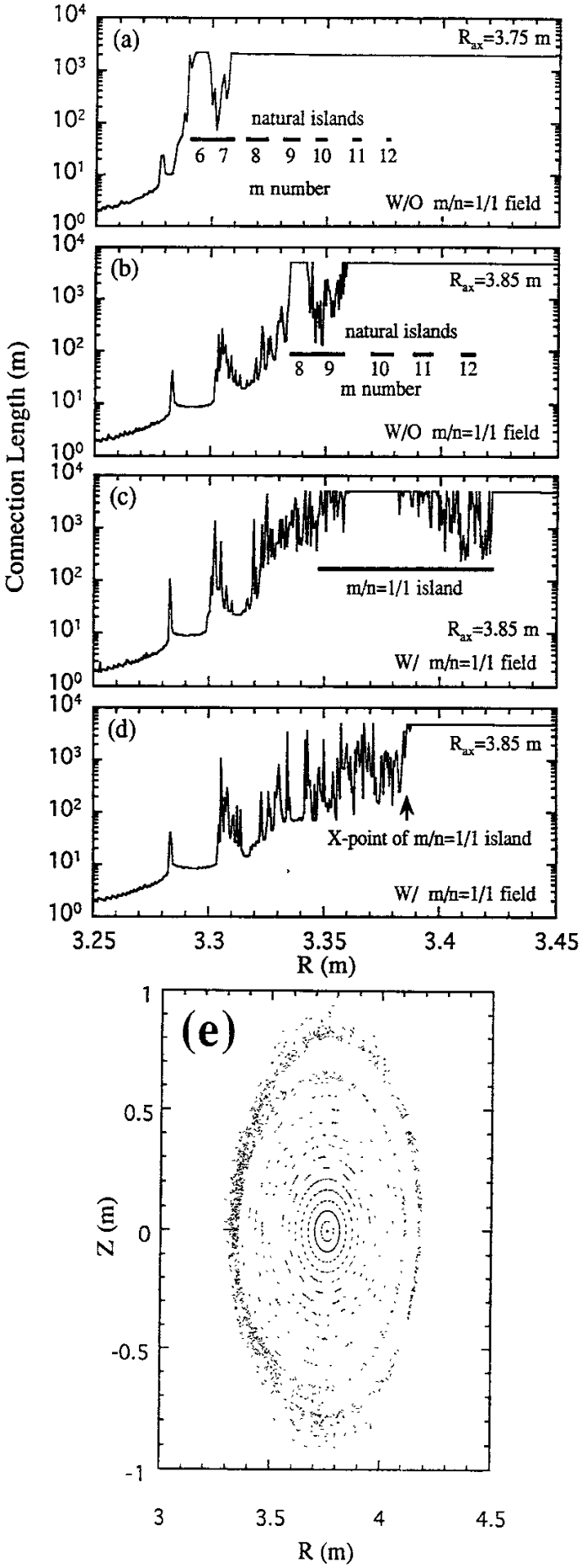
(a)
R_{ax}=3.75 m
natural islands
6 7 8 9 10 11 12
m number
W/O m/n=1/1 field
(b)
R_{ax}=3.85 m
natural islands
8 9 10 11 12
m number
W/O m/n=1/1 field
(c)
m/n=1/1 island
R_{ax}=3.85 m
W/ m/n=1/1 field
(d)
R_{ax}=3.85 m
X-point of m/n=1/1 island
W/ m/n=1/1 field
Connection Length (m)
R (m)
(e)
Z (m)
R (m)

Fig.5

Recent Issues of NIFS Series

NIFS-306 S. Murakami, M. Okamoto, N. Nakajima, K.Y. Watanabe, T. Watari, T. Mutoh, R. Kumazawa and T. Seki,
Monte Carlo Simulation for ICRF Heating in Heliotron/Torsatrons; Sep. 1994 (IAEA-CN-60/D-P-I-14)

NIFS-307 Y. Takeiri, A. Ando, O. Kaneko, Y. Oka, K. Tsumori, R. Akiyama, E. Asano, T. Kawamoto, T. Kuroda, M. Tanaka and H. Kawakami,
Development of an Intense Negative Hydrogen Ion Source with a Wide-Range of External Magnetic Filter Field; Sep. 1994

NIFS-308 T. Hayashi, T. Sato, H.J. Gardner and J.D. Meiss,
Evolution of Magnetic Islands in a Heliac; Sep. 1994

NIFS-309 H. Amo, T. Sato and A. Kageyama,
Intermittent Energy Bursts and Recurrent Topological Change of a Twisting Magnetic Flux Tube; Sep.1994

NIFS-310 T. Yamagishi and H. Sanuki,
Effect of Anomalous Plasma Transport on Radial Electric Field in Torsatron/Heliotron; Sep. 1994

NIFS-311 K. Watanabe, T. Sato and Y. Nakayama,
Current-profile Flattening and Hot Core Shift due to the Nonlinear Development of Resistive Kink Mode; Oct. 1994

NIFS-312 M. Salimullah, B. Dasgupta, K. Watanabe and T. Sato,
Modification and Damping of Alfvén Waves in a Magnetized Dusty Plasma; Oct. 1994

NIFS-313 K. Ida, Y. Miura, S -I. Itoh, J.V. Hofmann, A. Fukuyama, S. Hidekuma, H. Sanuki, H. Idei, H. Yamada, H. Iguchi, K. Itoh,
Physical Mechanism Determining the Radial Electric Field and its Radial Structure in a Toroidal Plasma; Oct. 1994

NIFS-314 Shao-ping Zhu, R. Horiuchi, T. Sato and The Complexity Simulation Group,
Non-Taylor Magnetohydrodynamic Self-Organization; Oct. 1994

NIFS-315 M. Tanaka,
Collisionless Magnetic Reconnection Associated with Coalescence of Flux Bundles; Nov. 1994

NIFS-316 M. Tanaka,
Macro-EM Particle Simulation Method and A Study of Collisionless Magnetic Reconnection; Nov. 1994

NIFS-317 A. Fujisawa, H. Iguchi, M. Sasao and Y. Hamada,
Second Order Focusing Property of 210° Cylindrical Energy Analyzer;

Nov. 1994

NIFS-318 T. Sato and Complexity Simulation Group,
Complexity in Plasma - A Grand View of Self- Organization; Nov. 1994

NIFS-319 Y. Todo, T. Sato, K. Watanabe, T.H. Watanabe and R. Horiuchi,
MHD-Vlasov Simulation of the Toroidal Alfvén Eigenmode; Nov. 1994

NIFS-320 A. Kageyama, T. Sato and The Complexity Simulation Group,
Computer Simulation of a Magnetohydrodynamic Dynamo II: Nov. 1994

NIFS-321 A. Bhattacharjee, T. Hayashi, C.C.Hegna, N. Nakajima and T. Sato,
Theory of Pressure-induced Islands and Self-healing in Three-dimensional Toroidal Magnetohydrodynamic Equilibria; Nov. 1994

NIFS-322 A. Iiyoshi, K. Yamazaki and the LHD Group,
Recent Studies of the Large Helical Device; Nov. 1994

NIFS-323 A. Iiyoshi and K. Yamazaki,
The Next Large Helical Devices; Nov. 1994

NIFS-324 V.D. Pustovitov
Quasisymmetry Equations for Conventional Stellarators; Nov. 1994

NIFS-325 A. Taniike, M. Sasao, Y. Hamada, J. Fujita, M. Wada,
The Energy Broadening Resulting from Electron Stripping Process of a Low Energy Au^- Beam; Dec. 1994

NIFS-326 I. Viniar and S. Sudo,
New Pellet Production and Acceleration Technologies for High Speed Pellet Injection System "HIPEL" in Large Helical Device; Dec. 1994

NIFS-327 Y. Hamada, A. Nishizawa, Y. Kawasumi, K. Kawahata, K. Itoh, A. Ejiri, K. Toi, K. Narihara, K. Sato, T. Seki, H. Iguchi, A. Fujisawa, K. Adachi, S. Hidekuma, S. Hirokura, K. Ida, M. Kojima, J. Koong, R. Kumazawa, H. Kuramoto, R. Liang, T. Minami, H. Sakakita, M. Sasao, K.N. Sato, T. Tsuzuki, J. Xu, I. Yamada, T. Watari,
Fast Potential Change in Sawteeth in JIPP T-IIU Tokamak Plasmas; Dec. 1994

NIFS-328 V.D. Pustovitov,
Effect of Satellite Helical Harmonics on the Stellarator Configuration; Dec. 1994

NIFS-329 K. Itoh, S-I. Itoh and A. Fukuyama,
A Model of Sawtooth Based on the Transport Catastrophe; Dec. 1994

NIFS-330 K. Nagasaki, A. Ejiri,
Launching Conditions for Electron Cyclotron Heating in a Sheared

Magnetic Field; Jan. 1995

NIFS-331 T.H. Watanabe, Y. Todo, R. Horiuchi, K. Watanabe, T. Sato,
An Advanced Electrostatic Particle Simulation Algorithm for Implicit Time Integration; Jan. 1995

NIFS-332 N. Bekki and T. Karakisawa,
Bifurcations from Periodic Solution in a Simplified Model of Two-dimensional Magnetoconvection; Jan. 1995

NIFS-333 K. Itoh, S.-I. Itoh, M. Yagi, A. Fukuyama,
Theory of Anomalous Transport in Reverse Field Pinch; Jan. 1995

NIFS-334 K. Nagasaki, A. Isayama and A. Ejiri
Application of Grating Polarizer to 106.4GHz ECH System on Heliotron-E; Jan. 1995

NIFS-335 H. Takamaru, T. Sato, R. Horiuchi, K. Watanabe and Complexity Simulation Group,
A Self-Consistent Open Boundary Model for Particle Simulation in Plasmas; Feb. 1995

NIFS-336 B.B. Kadomtsev,
Quantum Telegragh : is it possible?; Feb. 1995

NIFS-337 B.B.Kadomtsev,
Ball Lightning as Self-Organization Phenomenon; Feb. 1995

NIFS-338 Y. Takeiri, A. Ando, O. Kaneko, Y. Oka, K. Tsumori, R. Akiyama, E. Asano, T. Kawamoto, M. Tanaka and T. Kuroda,
High-Energy Acceleration of an Intense Negative Ion Beam; Feb. 1995

NIFS-339 K. Toi, T. Morisaki, S. Sakakibara, S. Ohdachi, T.Minami, S. Morita, H. Yamada, K. Tanaka, K. Ida, S. Okamura, A. Ejiri, H. Iguchi, K. Nishimura, K. Matsuoka, A. Ando, J. Xu, I. Yamada, K. Narihara, R. Akiyama, H. Idei, S. Kubo, T. Ozaki, C. Takahashi, K. Tsumori,
H-Mode Study in CHS; Feb. 1995

NIFS-340 T. Okada and H. Tazawa,
Filamentation Instability in a Light Ion Beam-plasma System with External Magnetic Field; Feb. 1995

NIFS-341 T. Watanbe, G. Gnudi,
A New Algorithm for Differential-Algebraic Equations Based on HIDM; Feb. 13, 1995

NIFS-342 Y. Nejoh,
New Stationary Solutions of the Nonlinear Drift Wave Equation; Feb. 1995

NIFS-343 A. Ejiri, S. Sakakibara and K. Kawahata,
Signal Based Mixing Analysis for the Magnetohydrodynamic Mode Reconstruction from Homodyne Microwave Reflectometry; Mar.. 1995

NIFS-344 B.B.Kadomtsev, K. Itoh, S.-I. Itoh
Fast Change in Core Transport after L-H Transition; Mar. 1995

NIFS-345 W.X. Wang, M. Okamoto, N. Nakajima and S. Murakami,
An Accurate Nonlinear Monte Carlo Collision Operator; Mar. 1995

NIFS-346 S. Sasaki, S. Takamura, S. Masuzaki, S. Watanabe, T. Kato, K. Kadota,
Helium I Line Intensity Ratios in a Plasma for the Diagnostics of Fusion Edge Plasmas; Mar. 1995

NIFS-347 M. Osakabe,
Measurement of Neutron Energy on D-T Fusion Plasma Experiments; Apr. 1995

NIFS-348 M. Sita Janaki, M.R. Gupta and Brahmananda Dasgupta,
Adiabatic Electron Acceleration in a Cnoidal Wave; Apr. 1995

NIFS-349 J. Xu, K. Ida and J. Fujita,
A Note for Pitch Angle Measurement of Magnetic Field in a Toroidal Plasma Using Motional Stark Effect; Apr. 1995

NIFS-350 J. Uramoto,
Characteristics for Metal Plate Penetration of a Low Energy Negative Muonlike or Pionlike Particle Beam: Apr. 1995

NIFS-351 J. Uramoto,
An Estimation of Life Time for A Low Energy Negative Pionlike Particle Beam: Apr. 1995

NIFS-352 A. Taniike,
Energy Loss Mechanism of a Gold Ion Beam on a Tandem Acceleration System: May 1995

NIFS-353 A. Nishizawa, Y. Hamada, Y. Kawasumi and H. Iguchi,
Increase of Lifetime of Thallium Zeolite Ion Source for Single-Ended Accelerator: May 1995

NIFS-354 S. Murakami, N. Nakajima, S. Okamura and M. Okamoto,
Orbital Aspects of Reachable β Value in NBI Heated Heliotron/Torsatrons; May 1995

NIFS-355 H. Sugama and W. Horton,
Neoclassical and Anomalous Transport in Axisymmetric Toroidal Plasmas with Electrostatic Turbulence; May 1995